Journal of Applied Physics

Calculation of the band structure, carrier effective mass, and the optical absorption properties of GaSbBi alloys

Cite as: J. Appl. Phys. **125**, 075705 (2019); https://doi.org/10.1063/1.5065573
Submitted: 11 October 2018 . Accepted: 04 January 2019 . Published Online: 20 February 2019

Subhasis Das, M. K. Bhowal, and S. Dhar

Journal of Applied Physics ARTICLE scitation.org/journal/jap

Calculation of the band structure, carrier effective mass, and the optical absorption properties of GaSbBi alloys

Cite as: J. Appl. Phys. **125**, 075705 (2019); doi: 10.1063/1.5065573
Submitted: 11 October 2018 · Accepted: 4 January 2019 ·
Published Online: 20 February 2019

Subhasis Das,[1,2,a)] M. K. Bhowal,[2] and S. Dhar[2]

AFFILIATIONS

[1]Centre for Research in Nanoscience and Nanotechnology, University of Calcutta, JD Sector-2, Salt Lake City, Kolkata 700098, India
[2]Department of Electronic Science, University of Calcutta, 92-APC Road, Kolkata 700009, India

Note: This paper is part of the Special Topic on: Highly Mismatched Semiconductors Alloys: from Atoms to Devices.
[a)]**E-mail:** subhasisdas700@gmail.com

ABSTRACT

The details of the electronic band structure of GaSbBi as functions of Bi mole fraction and along different symmetry directions of the crystal are calculated using a 14 band k.p model considering the band anti-crossing interaction between the valence band of the host III-V material and the Bi related impurity level resonant with the host. The effect of the lattice strain on the band structure as a result of incorporating a higher amount of Bi in the material is also studied. Variations of the bandgap energy, spin orbit split-off energy, band offsets, and the different sub-band energies are presented as functions of Bi content in GaSbBi as well as along the three symmetric k directions. Effective mass of the charge carriers and their dependence on Bi content is investigated. Furthermore, the intrinsic carrier concentration of the material as a function of Bi composition is evaluated. Finally, the optical absorption in the material is investigated considering the electronic transitions involving various valence sub bands and the conduction band.

INTRODUCTION

A number of experimental[1–4] and theoretical[5,6] works, carried out in the last few years, have investigated the details of the characteristic properties of the material GaSbBi, such as bandgap reduction with increasing Bi content and the large increase in spin orbit splitting energy. These characteristics make the material suitable for optoelectronic device applications in the mid-infrared spectral region.[7] Investigations have focused on the growth of $GaSb_{1-x}Bi_x$ epitaxial layers on GaSb substrates with different Bi compositions and on the study of the structural, electrical, and optical properties. Growth of the material has been observed by molecular beam epitaxy (MBE)[8] and liquid phase epitaxy (LPE).[1] Recently, the growth of GaSbBi/GaSb multiple quantum well structures and fabrication of laser diodes, based on the same, have been reported.[7] Carrier effective mass is known to have an important role in determining the optical and the electronic transport properties of semiconductors. Bi is reported to play a significant role on the value of the effective mass of the charge carriers in GaAsBi,[9] and a few experimental studies, done on GaAsBi, are related to the electron effective mass.[10,11]

In this article, we have presented a detailed calculation on the band structure of GaSbBi along different k-directions by using a 14 band k.p band anti-crossing (BAC) model. The model has been used to calculate the Bi-related bandgap reduction and the enhancement of the spin orbit splitting in GaSbBi as a function of Bi composition. In addition, carrier effective masses and the intrinsic carrier concentration as functions of Bi composition and along the symmetry k directions have been investigated which gave interesting information on the transport properties of the material. A theoretically simulated optical absorption coefficient for the inter band transitions in GaSbBi was found to be modified significantly by the perturbation of the localized Bi states into the valence band states of the host GaSb.

MATHEMATICAL METHODS

Calculation of the electronic band structure of $GaSb_{1-x}Bi_x$ was done by using the14 band k.p BAC model.[9] We have used a basic 8 band k.p Hamiltonian for the host GaSb material by considering a conduction band with the standard 6-band Luttinger-Kohn Hamiltonian describing heavy hole (HH), light hole (LH), and the spin orbit split-off bands as shown below[12]:

$$H_{8\times8} = \begin{bmatrix} ECB & 0 & -\frac{P_+}{\sqrt{2}} & \sqrt{\frac{2}{3}}P_z & \frac{P_-}{\sqrt{6}} & 0 & \frac{P_z}{\sqrt{3}} & \frac{P_-}{\sqrt{3}} \\ 0 & ECB & 0 & -\frac{P_+}{\sqrt{6}} & \sqrt{\frac{2}{3}}P_z & \frac{P_-}{\sqrt{2}} & \frac{P_+}{\sqrt{3}} & -\frac{P_z}{\sqrt{3}} \\ -\frac{P_+^*}{\sqrt{2}} & 0 & EHH & \alpha & \beta & 0 & \frac{i\alpha}{\sqrt{2}} & -i\sqrt{2}\beta \\ \sqrt{\frac{2}{3}}P_z & -\frac{P_+^*}{\sqrt{6}} & \alpha^* & ELH & 0 & \beta & \frac{iD}{\sqrt{2}} & i\sqrt{\frac{3}{2}}\alpha \\ \frac{P_-^*}{\sqrt{6}} & \sqrt{\frac{2}{3}}P_z & \beta^* & 0 & ELH & -\alpha & -i\sqrt{\frac{3}{2}}\alpha^* & \frac{iD}{\sqrt{2}} \\ 0 & \frac{P_-^*}{\sqrt{2}} & 0 & \beta^* & -\alpha^* & EHH & -i\sqrt{2}\beta^* & -\frac{i\alpha^*}{\sqrt{2}} \\ \frac{P_z}{\sqrt{3}} & \frac{P_+^*}{\sqrt{3}} & -\frac{i\alpha^*}{\sqrt{2}} & -\frac{iD}{\sqrt{2}} & i\sqrt{\frac{3}{2}}\alpha & i\sqrt{2}\beta & ESO & 0 \\ \frac{P_-^*}{\sqrt{3}} & -\frac{P_z}{\sqrt{3}} & i\sqrt{2}\beta^* & -i\sqrt{\frac{3}{2}}\alpha^* & -\frac{iD}{\sqrt{2}} & \frac{i\alpha}{\sqrt{2}} & 0 & ESO \end{bmatrix}. \quad (1)$$

Six localized p-like states of Bi atoms are represented by the diagonal matrix $H^{Bi}_{6\times6}$. It is constituted by the position of the heavy hole/light hole levels of Bi atom E_{Bi} and the corresponding spin-orbit split-off level $E_{Bi\text{-}SO}$, having the same basis function as that of the host GaSb, are added to extend the Hamiltonian to a 14×14 matrix.[13] The 8×8 matrix in Eq. (1) is modified as $H^{mod}_{8\times8}$ with the addition of the band offset terms $\Delta E_{CBM}x$ to the position of conduction band (ECB), $\Delta E_{VBM}x$ to the position of heavy and light holes (EHH, ELH), and $\Delta E_{SO}x$ to the position of spin orbit split off band (ESO). These are due to the linear change of the respective conduction, valence, and spin orbit split off band positions between the two end point binaries for different Bi contents according to the virtual crystal approximation (VCA). The terms constituting the Hamiltonian are described in Appendix A. The final expression for the 14×14 Hamiltonian matrix is as follows:[14]

$$H_{14\times14} = \begin{bmatrix} & & & & & & & & 0 & 0 & 0 & 0 & 0 & 0 \\ & & & & & & & & 0 & 0 & 0 & 0 & 0 & 0 \\ & & & & & & & & V_{Bi} & 0 & 0 & 0 & 0 & 0 \\ & & & & & & & & 0 & V_{Bi} & 0 & 0 & 0 & 0 \\ & & & H_{8\times8} & & & & & 0 & 0 & V_{Bi} & 0 & 0 & 0 \\ & & & & & & & & 0 & 0 & 0 & V_{Bi} & 0 & 0 \\ & & & & & & & & 0 & 0 & 0 & 0 & V_{Bi} & 0 \\ & & & & & & & & 0 & 0 & 0 & 0 & 0 & V_{Bi} \\ 0 & 0 & V_{Bi} & 0 & 0 & 0 & 0 & 0 & E_{Bi} & 0 & 0 & 0 & 0 & 0 \\ 0 & 0 & 0 & V_{Bi} & 0 & 0 & 0 & 0 & 0 & E_{Bi} & 0 & 0 & 0 & 0 \\ 0 & 0 & 0 & 0 & V_{Bi} & 0 & 0 & 0 & 0 & 0 & E_{Bi} & 0 & 0 & 0 \\ 0 & 0 & 0 & 0 & 0 & V_{Bi} & 0 & 0 & 0 & 0 & 0 & E_{Bi} & 0 & 0 \\ 0 & 0 & 0 & 0 & 0 & 0 & V_{Bi} & 0 & 0 & 0 & 0 & 0 & E_{Bi-SO} & 0 \\ 0 & 0 & 0 & 0 & 0 & 0 & 0 & V_{Bi} & 0 & 0 & 0 & 0 & 0 & E_{Bi-SO} \end{bmatrix}. \quad (2)$$

Here, V_{Bi} represents the interaction energy between the iso-electronic localized state of Bi and the three p like states of the host GaSb valance band. Furthermore, the coupling term for Bi is denoted as $V_{Bi} = C_{Bi}\sqrt{x}$, where x is the Bi mole fraction and C_{Bi} is a measure of the strength of the interaction. The localized states of the Bi atom are represented by an additional diagonal matrix and are constituted by the localized Bi position of energy levels E_{Bi} and E_{Bi-SO}. The lattice constant of $GaSb_{1-x}Bi_x$ is obtained from Vegard's law as a linear interpolation of the lattice constant of the two end point binaries as

$$a_{GaSb_{1-x}Bi_x} = (1-x)a_{GaSb} + x\, a_{GaBi}, \quad (3)$$

where the value of a_{GaBi} is 6.324 Å[15] and that of a_{GaSb} is 6.095 Å.[16] All the BAC parameters, used to calculate the band structure, are listed in Table IV. Band structure is obtained by diagonalization of the matrix $H_{14\times14}$ and the same is used to calculate the effective mass m^* using the 14 band BAC model at the Γ point in the non-equivalent high symmetry **k**-direction (Λ, Δ, and Σ). We can get the heavy hole (m^*_{hh+}), light hole (m^*_{lh+}), spin-orbit splitting (m^*_{SO+}), and the electron effective mass (m^*_{cbe}) from the second derivative of the energy sub-bands near the Brillouin zone centre.

RESULTS AND DISCUSSIONS

Figure 1(a) shows the electronic band structure of $GaSb_{1-x}Bi_x$, calculated for x = 0.125, near the Γ point in the Λ, Δ, and Σ high symmetry non-equivalent **k** directions by using the14 band BAC model at 300 K. This model has been used to calculate the band structure up to 30% of the total length of each high symmetry directions. Unit of the length is taken as $2\pi/a$, where "a" is the lattice constant of GaSbBi, determined by the linear interpolation of the two end point binaries. The origin of the energy axis is taken at the top of the valence band (valence band maximum). The interaction between the host valance band matrix and the nearby situated Bi energy levels E_{Bi} and $E_{Bi\text{-}SO}$ causes splitting of the heavy hole (HH), light hole (LH), and the spin-orbit splitting (SO) bands while the conduction band (CB) is left unaffected. All these exercises result in the formation of the bands, E_{CB}, $E_{HH^+_-}$, E_{LH^+}, and $E_{SO^+_-}$, and a degenerate valence band is predicted at the Γ point.

The band structure of GaSb is calculated by the k.p method using an eight band second order Kane model which is added in Fig. 1(a) for comparison with the band structure of GaSbBi. From dispersion relations, it is also found that the conduction band of GaSbBi changes with nearly the same fashion as that of GaSb. On the other hand, values of valence sub bands, like E_{HH+}, E_{LH+}, E_{SO+}, and E_{HH-}, change away from GaSb valence band for larger k values in all directions. However, the k dependence of E_{LH-} and E_{SO-} shows a different nature with respect to that of GaSb but for larger k values where they follow each other.

Energy sub band levels are plotted for Bi contents up to 14 at. % in Fig. 1(b). The BAC model predicts that for higher Bi content, E_{CB} and $E_{HH+/LH+}$ change more sharply than the other sub bands. Due to the incorporation of high mole fraction Bi (12.5%) in GaSb, conduction band minimum (CBM) decreases by 351.1 meV and there is an increase of the

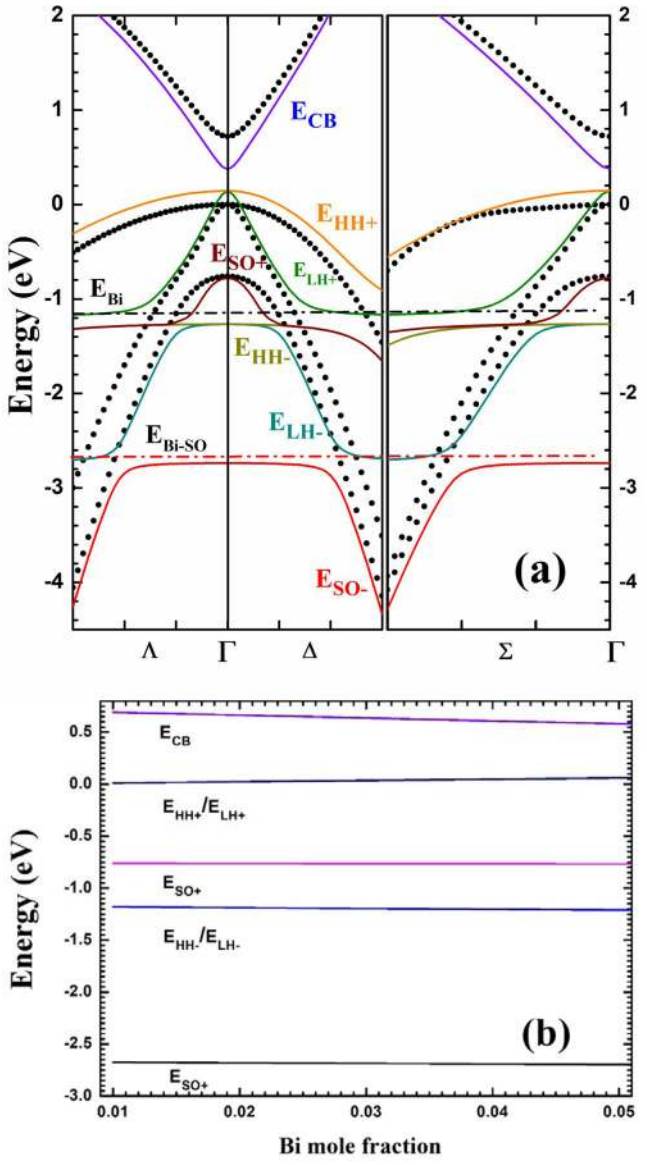

FIG. 1. (a) The electronic band structure of $GaSb_{0.875}Bi_{0.125}$ calculated by the 14 band k.p BAC model near the Γ point in three high symmetry directions Δ, Λ, and Σ shows the conduction band, heavy hole, light hole, and the spin-orbit split-off hole levels and their comparison with the same parameters for GaSb (solid dots) calculated from the 8 band k.p model. (b) Variation of the different energy sub-bands with increasing Bi content.

valance band maximum (VBM) by 146.2 meV. These amount to a gross bandgap reduction of 492.8 meV corresponding to a bandgap reduction rate of ~39 meV per percent of Bi incorporation. This value is close to the recent experimental value of 35 meV/% Bi.[3] The spin-orbit splitting band (SO) moves downward by 20 meV. Figure 1(a) indicates that Bi causes an upward shift of the VBM, whereas the CBM and the spin orbit splitting energy band show a downward movement.

The dependence of E_g on Bi mole fraction x in $GaSb_{1-x}Bi_x$ is obtained from BAC model as

$$E_g(x) = 0.72(1-x) - 2.63x - 0.67x\,(1-x). \quad (4)$$

From the Bi dependence of the bandgap energy, a bowing parameter of 0.67 eV is obtained which indicates that the values of E_g from calculations, based on the BAC model, are different from that obtained from a linear interpolation between two end point binaries GaSb and GaBi.

At room temperature, the value of Δ_{SO} is sufficiently higher than E_g which increases further with an increase in the Bi content in the material with a corresponding decrease in E_g. This property reduces the non-radiative Auger recombination processes, which is expected to make the material an attractive candidate for the fabrication of laser diodes. The spin orbit splitting energy dependence on Bi mole fraction x of $GaSb_{1-x}Bi_x$ is obtained from the BAC model as

$$\Delta_{SO}(x) = 0.76(1-x) + 1.43x + 0.71x\,(1-x). \quad (5)$$

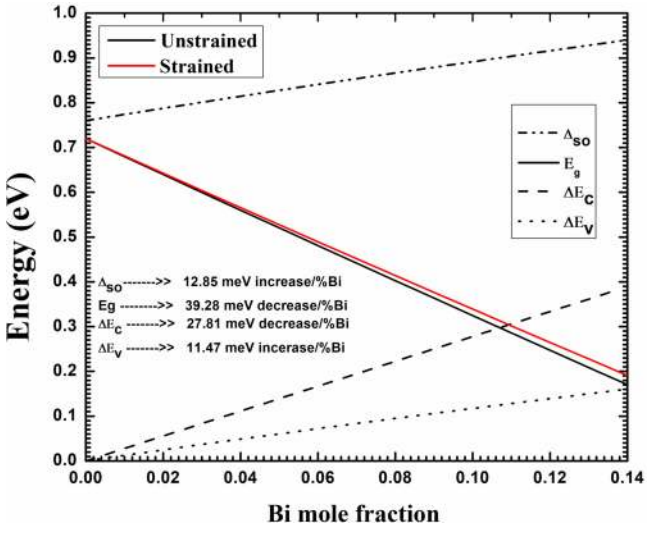

FIG. 2. Dependence of Bi mole fraction on bandgap (E_g), spin orbit splitting energy (E_{SO}), and the changes in the conduction band edge (ΔE_C) and the valence band edge (ΔE_V) in GaSbBi with respect to that for GaSb.

From this equation, it is found that Δ_{SO} changes nearly by 12 meV/% Bi for GaSbBi. Again ΔE_{CB} and ΔE_{VB}, respectively, are the relative conduction band and valence band energy positions of GaSbBi with respect to that of GaSb. ΔE_{CB} changes linearly with Bi content according to the VCA. BAC modal estimates a functional relationship of ΔE_{VB} with Bi mole fraction x as

$$\Delta E_{VB}(x) = 2.16 \times 10^{-4}(1-x) + 0.58x + 0.66x\,(1-x). \quad (6)$$

Figure 2 presents the variation of all the above parameters with Bi content in the material.

Due to the incorporation of a higher amount of Bi in the lattice, compressive strain, generated at the interface of GaSbBi and GaSb, plays an important role. The strain causes a splitting of the heavy hole and the light hole levels at the zone centre which was found experimentally using photoreflectance (PR) techniques.[2]

To consider the effect of strain on the Hamiltonian in Eq. (1), hydrostatic components of strain are added to both the conduction and the valence bands. Additionally, shear component of strain breaks the valence band degeneracy by separating heavy hole and light hole energy levels as[17]

$$\begin{aligned} ECB_{strain} &= ECB_{unstrain} + \delta E_{CB}^{hy}, \\ EHH_{strain} &= EHH_{unstrain} + \delta E_{VB}^{hy} - \frac{1}{2}\delta E_S, \\ ELH_{strain} &= ELH_{unstrain} + \delta E_{VB}^{hy} + \frac{1}{2}\delta E_S. \end{aligned} \quad (7)$$

Here δE_{CB}^{hy} and δE_{VB}^{hy} are the hydrostatic components of strain which, respectively, tend to shift the conduction band and valence band. δE_S is the shearing component of strain. Detailed calculations of these strain components are described in Appendix B.

Using the strain modified Hamiltonian, we have calculated the band structure of GaSbBi with 14 at. % Bi and compared it with the unstrained band structure in Fig. 3. We also compared the variation of the bandgap E_g with changes in the Bi at. % for unstrained and strained GaSbBi in Fig. 2. It is observed that E_g in both cases is comparable up to about 6 at. % Bi. For further rise in the Bi content, E_g shows a decrease for the unstrained case with respect to that calculated considering strain. At 14 at. % Bi content, the difference is as high as 200 meV and the rate of reduction of E_g is decreased from 39.28 meV to 37.85 meV per at. % Bi. These results are important for the design of heterostructure and quantum well devices. Bandgap reduction of GaSbBi per %Bi obtained from the literature are illustrated in Table I.

A knowledge of the electron effective mass in GaSbBi as a function of Bi content is important for understanding the carrier transport in the material and technologically a key parameter for the design of devices. Effective masses are

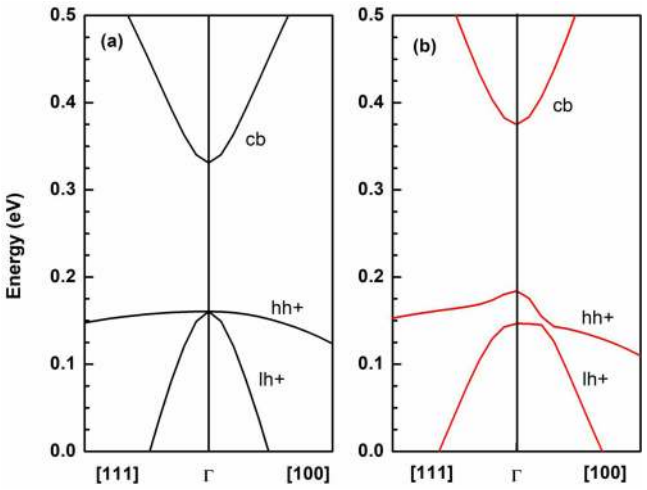

FIG. 3. Electronic band structure of (a) unstrained $GaSb_{0.86}Bi_{0.14}$ and (b) strained $GaSb_{0.86}Bi_{0.14}$ near the Brillouin zone centre.

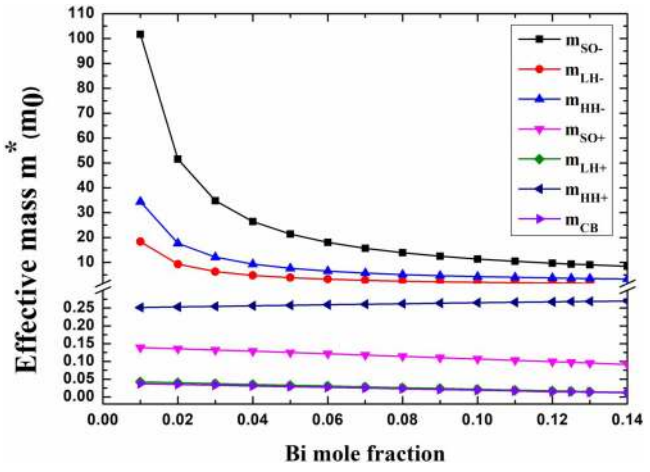

FIG. 4. Variation of effective mass in different energy sub-bands of GaSbBi with an increase in Bi compositions.

calculated from the band structure near the Brillouin zone centre by using the relation

$$\frac{1}{m^*(k)} = \frac{1}{\hbar^2 k}\left|\frac{dE(k)}{dk}\right|, \tag{8}$$

where E(k) values are related to the different energy sub-bands including the conduction band and the six degenerate valence bands and are obtained from the interaction of the host valence bands with the Bi energy levels. Figure 4 shows the dependence of different sub-band effective masses in GaSbBi on Bi mole fraction up to a maximum of 0.14. For GaSb (with no Bi), different values of the electron and the hole effective masses were calculated by solving the standard 8-band k.p model, and the results are shown in Table II.

Effective masses display a change in their values with increasing Bi content in GaSb. Figure 4 shows that the values of the lower sub-band hole effective masses m_{SO-}, m_{LH-}, and m_{HH-} are some ten times the rest mass m_0, and these are quite heavier than the upper sub-band hole effective masses m_{SO+}, m_{LH+}, and m_{HH+}. The value of m_{SO-} is very high at low value of Bi in the material and rapidly falls and saturates close to a value ~4-6 at. % of Bi. However, in spite of the values being very high compared to the upper sub-band effective masses, they are not expected to contribute significantly to the transport properties. Similar variation is observed for m_{HH-} and m_{LH-} though the maximum values are relatively low. Variation of the upper sub band hole effective masses and that of the electron effective mass are somewhat insignificant in the entire range of the Bi mole fraction investigated. Hence, we are mostly interested in the values of m_{SO+}, m_{LH+}, m_{HH+} and m_{CB}, and their dependence on the Bi content along the symmetry directions are plotted in Fig. 5. From this figure, the approximate changes in the conduction and valence band effective masses with Bi along three symmetric directions are calculated and listed in Table III.

To our knowledge, there are no such experimental results of carrier effective masses of GaSbBi reported. The accuracy of the bandgap reduction and the effective mass

TABLE I. Rate of reduction of the bandgap energy E_g per % Bi in GaSbBi.

Procedure	Bandgap Reduction/%Bi	Reference
Photoluminescence	35 meV	Wang[18]
Absorption	35 meV	Rajpalke *et al.*[3]
Absorption	32 meV (up to 4.5 at. % Bi)	Rajpalke *et al.*[4]
Ab initio calculation	35.6 meV (<5 at. % Bi)	Polak *et al.*[5]
Photoreflectance	30 meV (<4.2 at. % Bi)	Kopaczek *et al.*[2]
Photoluminescence	28 meV (up to 14 at. %Bi)	Delorme *et al.*[19]
Valence band anticrossing model	40.2 meV	Samajdar *et al.*[20]
14 × 14 band anticrossing model	39.2 meV (without strain) 37.8 meV (with strain)	This work

TABLE II. Effective mass of electrons and holes in GaSb, calculated from 8 band k.p model.

Electron	Heavy hole	Light hole	Spin orbit split off hole
0.039 m_0	0.25 m_0	0.048 m_0	0.138 m_0

variation obtained depend mostly on the selection of the different BAC parameters used in the calculation which are being listed in Table IV.

The parameter E_{Bi} is the position of Bi level below the valence band edge of GaSb and was calculated using the position of the Bi-energy level with respect to GaAs valence band edge[13] and the valence band offset between GaSb and GaAs.[16] Another important parameter is C_{Bi} which is a fitting parameter. C_{Bi} has been selected here by fitting the experimental bandgap data of GaSbBi as a function of Bi content reported in different studies.[3,18]

The valence band offset ΔE_{VBM} was determined from the comparison of valence band edge energies of GaSb and GaBi taken from Refs. 16 and 21. Similarly, conduction band offset ΔE_{CBM} is calculated by putting the bandgap energies of GaSb and GaBi from Refs. 16 and 20. Finally, spin orbit split-off band offset was estimated from the theoretical value of the GaBi spin orbit splitting energy.[22]

Using these BAC parameters, our calculated result shows good agreement with the majority of other works listed in Table I.

TABLE III. Change in the value of the electron and the hole effective masses per % Bi along the different high symmetry k directions.

Effective mass	Δ	Λ	Σ
m_{CB}	-1.9628×10^{-3}	-1.9607×10^{-3}	-1.9592×10^{-3}
m_{HH+}	1.2964×10^{-3}	1.8385×10^{-3}	3.7×10^{-3}
m_{LH+}	-2.1185×10^{-3}	-1.90357×10^{-3}	-1.84714×10^{-3}
m_{SO+}	-3.3907×10^{-3}	-3.39714×10^{-3}	-3.3985×10^{-3}

The calculated values of the carrier effective masses were next used to obtain the intrinsic carrier concentration (n_i) in GaSbBi as a function of Bi content using the relation

$$n_i(x, T) = 2.5 \times 10^{19} m_C^*(x)^{3/4} m_V^*(x)^{3/4} \left(\frac{T}{300}\right)^{3/2} e^{-\frac{E_g(x,T)}{2k_\beta T}}, \quad (9)$$

where m_C^* and m_V^*, respectively, are the density of state effective masses of conduction band and valence band and are given by m_{CB} and $\left\{ {m_{HH+}^*}^{3/2} + {m_{LH+}^*}^{3/2} + \left[m_{SO+}^* \exp\left(-\frac{\Delta_{SO}}{kT}\right)\right]^{3/2} \right\}^{2/3}$.[23] The results of our calculations are being presented in Fig. 6.

For GaSb, n_i has a value of $\sim 8 \times 10^{11}$ cm^{-3} which according to our calculated results in Fig. 8 increases with the incorporation of Bi, and this increment is doubled per at. % Bi. The obvious reason is the lowering of bandgap due to Bi addition.

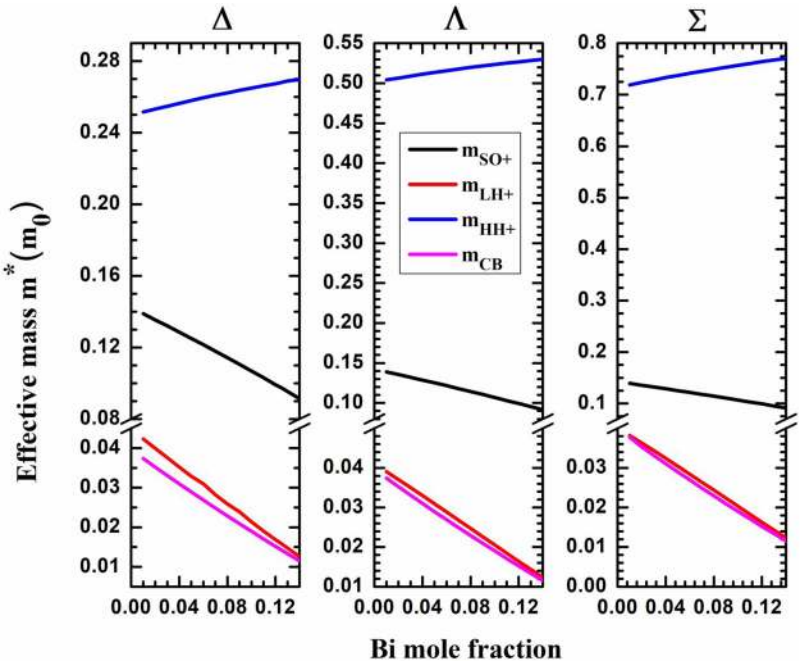

FIG. 5. Values of carrier effective mass along the symmetry k directions: Δ, Λ, and Σ in k-space for some important specific sub-bands like conduction band E_{CB} (m_{CB}^*), heavy holes E_{HH+} (m_{HH+}^*), light holes E_{LH+} (m_{LH+}^*) and spin orbit split off holes E_{SO+}(m_{SO+}^*).

TABLE IV. Parameters used in BAC model.

E_G(eV)	E_P(eV)	E_{Bi}(eV)	E_{Bi-SO}(eV)	C_{Bi}	ΔE_{CBM}(eV)	ΔE_{VBM}(eV)	ΔE_{SO}(eV)	Δ_{SO}(eV)	γ_1^L	γ_2^L	γ_3^L
0.72	27	−1.17	−2.67	1.01	−2.78	0.38	−1.06	0.76	13.4	4.6	6

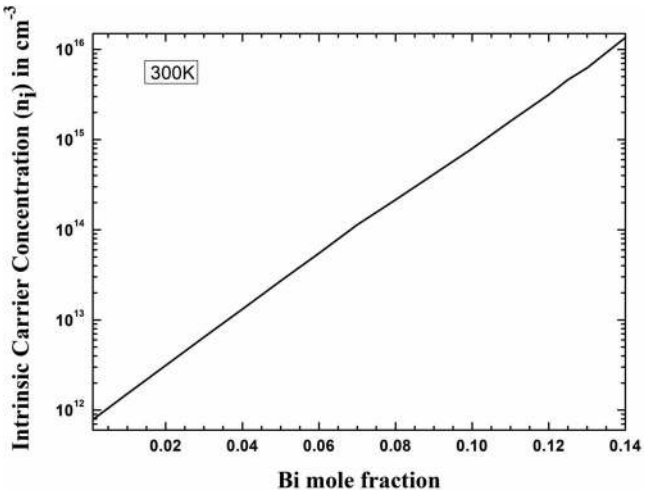

FIG. 6. Variation of intrinsic carrier concentration of GaSbBi as a function of Bi mole fraction in GaSbBi.

For investigation of the optical absorption properties of GaSbBi, we used the electronic band structure obtained from the BAC model using the procedure prescribed by Perlin *et al.*[24] The absorption coefficient is given as[25]

$$\alpha(h\nu) \propto \sum_{c,v} \frac{|P_{cv}|^2 J_{cv}(h\nu)}{h\nu}, \tag{10}$$

where P_{cv} is the momentum matrix element for the optical transition, obtained from the BAC model. J_{cv} is the optical joint density of state, given by

$$J_{cv} \propto \int \delta[E_c(k) - E_v(k) - \hbar\omega]dk. \tag{11}$$

E_c is the conduction band energy of GaSbBi and E_v represents the different valence sub-bands formed by the interactions of HH, LH, and SO with the localized Bi levels. The total absorption coefficient is obtained as the sum of the different

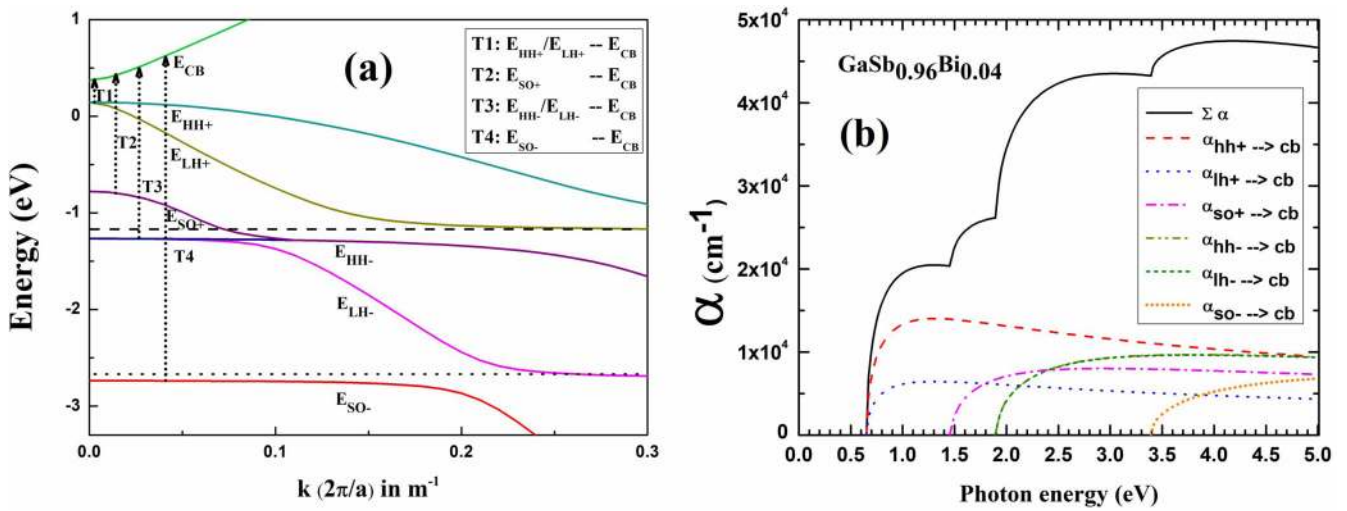

FIG. 7. (a) Band dispersion in GaSbBi and the possible transitions between the conduction band and the valence sub-bands. (b) Calculated absorption spectrum of $GaSb_{0.96}Bi_{0.04}$ where the total absorption is shown as a result of the different sub band absorption components.

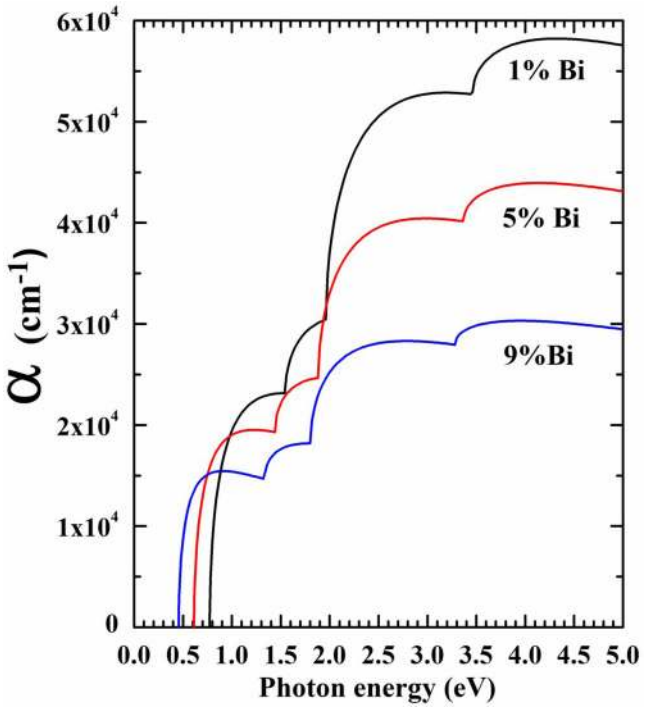

FIG. 8. Absorption coefficient vs photon energy for three different Bi content in GaSbBi.

sub-band absorptions.[26] Figure 7(a) shows the various electronic transitions involved in the absorption process.

The total optical absorption in GaSbBi is described by six interband transitions, as shown in Fig. 7(b). The total absorption is associated with four different valence sub band transitions indicated by the steps in the absorption spectrum as is observed. In Fig. 8, the spectra are presented for three different Bi content in the material and indicate that increased Bi tends to reduce the absorption in the material.

CONCLUSION

We have modified the usual 12 band k.p valence band anticrossing model to a 14 band k.p model by taking into consideration the conduction band along with the valence sub bands to calculate the band structure and the related parameters of GaSbBi as a function of Bi content and along the different high symmetry k directions. We have considered the effect of compressive strain emanating from the introduction of Bi in GaSb and calculated the band structure near the Brillouin zone for both strained and unstrained cases for high Bi content in GaSbBi. The variation of carrier effective masses in different sub-band energy levels and along the symmetric k directions and their dependence on Bi have been obtained. The calculated values of the effective masses have been used to further calculate the intrinsic carrier concentration in the material as a function of Bi content. Finally, we have calculated the values of the absorption coefficient in the material for different Bi compositions and obtained the details of the transitions involved in the absorption process.

ACKNOWLEDGMENTS

Subhasis Das acknowledges financial support obtained through a Senior Research Fellowship from the University Grants Commission, Government of India.

APPENDIX A: TERMS USED IN HAMILTONIAN (1)

$$\mathrm{ECB} = \mathrm{E_g} + \frac{\hbar^2}{2m_0}\left[\frac{1}{m_e^*} - \frac{E_p}{3}\left(\frac{2}{E_g} + \frac{1}{E_g + \Delta_{SO}}\right)\right] \times (k_x^2 + k_y^2 + k_z^2) + \Delta E_{CBM}x,$$

$$\mathrm{EHH} = \frac{-\hbar^2}{2m_0}[(k_x^2 + k_y^2)(\gamma_1 + \gamma_2) + k_z^2(\gamma_1 - 2\gamma_2)] + \Delta E_{VBM}x,$$

$$\mathrm{ELH} = \frac{-\hbar^2}{2m_0}[(k_x^2 + k_y^2)(\gamma_1 - \gamma_2) + k_z^2(\gamma_1 + 2\gamma_2)] + \Delta E_{VBM}x,$$

$$\mathrm{ESO} = \frac{1}{2}(L + H) - \Delta_{SO} + \Delta E_{SO}x,$$

$$P_{\pm} = P(k_x \pm i\, k_y),$$

$$P_z = P\, k_z,$$

$$\alpha = \frac{\hbar^2}{2m_0} 2\sqrt{3}[k_z(k_x - i\, k_y)\gamma_3],$$

$$\beta = \frac{\hbar^2}{2m_0}\sqrt{3}[(k_x^2 - k_y^2)\gamma_2 - 2ik_xk_y\gamma_3],$$

$$D = L - H.$$

E_g is the unstrained bandgap of GaSb and P is the Kane matrix element in terms of energy unit as

$$E_P = \frac{2\, m_0}{\hbar^2} P^2.$$

The valence band parameters used in the 8-band Hamiltonian is different from Luttinger parameters used in the 6 × 6 Hamiltonian, since the conduction band is now treated exactly in the 8 × 8 Hamiltonian and must be subtracted off the original Luttinger parameters. These parameters are called modified Luttinger parameters and are related to

Luttinger parameters by the following relation:[1]

$$\gamma_1 = \gamma_1^L - \frac{E_P}{3E_g},$$

$$\gamma_2 = \gamma_2^L - \frac{E_P}{6E_g},$$

$$\gamma_3 = \gamma_3^L - \frac{E_P}{6E_g}.$$

APPENDIX B: STRAIN COMPONENTS

$$\delta E_{CB}^{hy} = -2\, a_c \left(1 - \frac{C_{12}}{C_{11}}\right)\varepsilon,$$

$$\delta E_{VB}^{hy} = -2\, a_v \left(1 - \frac{C_{12}}{C_{11}}\right)\varepsilon,$$

$$\delta E_S = -b\left(1 + \frac{2C_{12}}{C_{11}}\right)\varepsilon.$$

Here a_c and a_v are hydrostatic deformation potentials for the conduction and valence band, respectively, and b is the axial deformation potential. C_{11} and C_{12} are the elastic constants. Values of these constants for GaSbBi are calculated by the linear interpolation between the parent binaries i.e., GaSb and GaBi.

The strain in the layer ε is given by

$$\varepsilon = \frac{a_{GaSbBi} - a_{GaSb}}{a_{GaSb}}.$$

REFERENCES

[1]S. K. Das, T. D. Das, S. Dhar, M. De La Mare, and A. Krier, "Near infrared photoluminescence observed in dilute GaSbBi alloys grown by liquid phase epitaxy," Infrared Phys. Technol. **55**(1), 156–160 (2012).
[2]J. Kopaczek, R. Kudrawiec, W. M. Linhart, M. K. Rajpalke, K. M. Yu, T. S. Jones, M. J. Ashwin, J. Misiewicz, and T. D. Veal, "Temperature dependence of the band gap of $GaSb_{1-x}Bi_x$ alloys with $0<x\leq0.042$ determined by photoreflectance," Appl. Phys. Lett. **103**(26), 261907 (2013).
[3]M. K. Rajpalke, W. M. Linhart, M. Birkett, K. M. Yu, J. Alaria, J. Kopaczek, R. Kudrawiec, T. S. Jones, M. J. Ashwin, and T. D. Veal, "High Bi content GaSbBi alloys," J. Appl. Phys. **116**(4), 043511 (2014).
[4]J. Kopaczek, R. Kudrawiec, W. Linhart, M. Rajpalke, T. Jones, M. Ashwin, and T. Veal, "Low-and high-energy photoluminescence from $GaSb_{1-x}Bi_x$ with $0<x\leq0.042$," Appl. Phys. Express **7**(11), 111202 (2014).
[5]M. P. Polak, P. Scharoch, R. Kudrawiec, J. Kopaczek, M. J. Winiarski, W. M. Linhart, M. K. Rajpalke *et al.*, "Theoretical and experimental studies of electronic band structure for $GaSb_{1-x}Bi_x$ in the dilute Bi regime," J. Phys. D Appl. Phys. **47**(35), 355107 (2014).
[6]M. P. Polak, P. Scharoch, and R. Kudrawiec, "First-principles calculations of bismuth induced changes in the band structure of dilute Ga–V–Bi and In–V–Bi alloys: Chemical trends versus experimental data," Semicond. Sci. Technol. **30**(9), 094001 (2015).
[7]O. Delorme, L. Cerutti, E. Luna, G. Narcy, A. Trampert, E. Tournié, and J.-B. Rodriguez, "GaSbBi/GaSb quantum well laser diodes," Appl. Phys. Lett. **110**(22), 222106 (2017).
[8]Y. Song, S. Wang, I. S. Roy, P. Shi, and A. Hallen, "Growth of $GaSb_{1-x}Bi_x$ by molecular beam epitaxy," J. Vac. Sci. Technol. B **30**(2), 02B114 (2012).
[9]M. M. Habchi, A. Ben Nasr, A. Rebey, and B. El Jani, "Theoretical study of optoelectronic properties of $GaAs_{1-x}Bi_x$ alloys using valence band anti-crossing model," Infrared Phys. Technol. **67**, 531–536 (2014).
[10]B. Fluegel, R. N. Kini, A. J. Ptak, D. Beaton, K. Alberi, and A. Mascarenhas, "Shubnikov-de Haas measurement of electron effective mass in $GaAs_{1-x}Bi_x$," Appl. Phys. Lett. **99**(16), 162108 (2011).
[11]G. Pettinari, O. Drachenko, R. B. Lewis, and T. Tiedje, "Electron effective mass enhancement in Ga (As Bi) alloys probed by cyclotron resonance spectroscopy," Phys. Rev. B **94**(23), 235204 (2016).
[12]S. T. Ng, W. J. Fan, Y. X. Dang, and S. F. Yoon, "Comparison of electronic band structure and optical transparency conditions of $In_x Ga_{1-x} As_{1-y} N_y$/Ga As quantum wells calculated by 10-band, 8-band, and 6-band $k \cdot p$ models," Phys. Rev. B **72**(11), 115341 (2005).
[13]K. Alberi, J. Wu, W. Walukiewicz, K. M. Yu, O. D. Dubon, S. P. Watkins, C. X. Wang, X. Liu, Y.-J. Cho, and J. Furdyna, "Valence-band anticrossing in mismatched III-V semiconductor alloys," Phys. Rev. B **75**(4), 045203 (2007).
[14]S. Imhof, C. Bückers, A. Thränhardt, J. Hader, J. V. Moloney, and S. W. Koch, "Microscopic theory of the optical properties of Ga (AsBi)/GaAs quantum wells," Semicond. Sci. Technol. **23**(12), 125009 (2008).
[15]S. Francoeur, M. J. Seong, A. Mascarenhas, S. Tixier, M. Adamcyk, and T. Tiedje, "Band gap of $GaAs_{1-x}$ Bi_x, $0<x<3.6\%$," Appl. Phys. Lett. **82**(22), 3874–3876 (2003).
[16]I. Vurgaftman, J. R. Meyer, and L. R. Ram-Mohan, "Band parameters for III–V compound semiconductors and their alloys," J. Appl. Phys. **89**(11), 5815–5875 (2001).
[17]M. Gladysiewicz, R. Kudrawiec, and M. S. Wartak, "8-band and 14-band kp modeling of electronic band structure and material gain in Ga (In) AsBi quantum wells grown on GaAs and InP substrates," J. Appl. Phys. **118**(5), 055702 (2015).
[18]S. Wang, "Dilute III-PBi and III-SbBi for IR applications," in 2016 18th International Conference on Transparent Optical Networks (ICTON) (IEEE, 2016), pp. 1-3.
[19]O. Delorme, L. Cerutti, E. Tournié, and J.-B. Rodriguez, "Molecular beam epitaxy and characterization of high Bi content GaSbBi alloys," J. Cryst. Growth **477**, 144–148 (2017).
[20]D. P. Samajdar, T. D. Das, and S. Dhar, "Valence band anticrossing model for $GaSb_{1-x}Bi_x$ and $GaP_{1-x}Bix$ using kp method," Mater. Sci. Semicond. Process. **40**, 539–542 (2015).
[21]M. Usman, C. A. Broderick, A. Lindsay, and E. P. O'Reilly, "Tight-binding analysis of the electronic structure of dilute bismide alloys of GaP and GaAs," Phys. Rev. B **84**(24), 245202 (2011).
[22]P. Carrier and S.-H. Wei, "Calculated spin-orbit splitting of all diamond like and zinc-blende semiconductors: Effects of p 1/2 local orbitals and chemical trends," Phys. Rev. B **70**(3), 035212 (2004).
[23]M. A. Green, "Intrinsic concentration, effective densities of states, and effective mass in silicon," J. Appl. Phys. **67**(6), 2944–2954 (1990).
[24]P. Perlin, P. Wiśniewski, C. Skierbiszewski, T. Suski, E. Kamińska, S. G. Subramanya, E. R. Weber, D. E. Mars, and W. Walukiewicz, "Interband optical absorption in free standing layer of $Ga_{0.96}In_{0.04}As_{0.99}N_{0.01}$," Appl. Phys. Lett. **76**(10), 1279–1281 (2000).
[25]P. Bhattacharya, *Semiconductor Optoelectronic Devices*, 2nd ed. (Prentice Hall, 1997).
[26]M. Seifikar, E. P. O'Reilly, and S. Fahy, "Optical absorption of dilute nitride alloys using self-consistent Green's function method," Nanoscale Res. Lett. **9**(1), 51 (2014).